Phonon Scattering from Substitutional Impurities and Lattice Defects in Silver Chloride†

CHEUK-KIN CHAU* AND MILES V. KLEIN
Department of Physics and Materials Research Laboratory, University of Illinois, Urbana, Illinois 61801
(Received 20 October 1969)

The thermal conductivity of silver chloride doped with varying concentrations of eight impurities—Li^+, Na^+, K^+, Rb^+, Cu^+, Cu^{++}, Br^-, and I^-—was measured in the temperature range 1.2 to 80°K. Only in the quenched, heavily lithium-doped crystal was a definite thermal conductivity dip observed. The strong low-temperature depressions in the thermal conductivity of the Cu^{++}-doped crystals suggest a possible resonance below 1°K. The far-infrared absorption of some of the doped crystals was measured from 33 to 105 cm^{-1} at 7°K. Impurity-induced absorption peaks were observed in all cases, except for the rubidium-doped crystal, where the concentration was perhaps too low to give rise to an induced absorption. The thermal conductivity of pure silver-chloride crystals subjected to various heat and surface treatments was also measured. The results suggest that phonon scattering is mainly due to dislocations and that diffuse boundary scattering is perhaps due to dynamical dislocation loops beneath the surface. The thermal conductivity curve of the pure single crystal was fitted by using the Debye thermal conductivity integral. Because of the existence of many low-energy critical points, a two-group-velocity model was employed. A relatively strong normal-process relaxation rate suggests that anharmonicity may be important.

I. INTRODUCTION

THE low-temperature thermal conductivity of dielectric crystals containing imperfections has been studied extensively from both an experimental and a theoretical viewpoint. The scattering caused by imperfections such as external boundaries,[1–3] isotopes,[4–6] and dislocations,[7–9] in chemically pure crystals has been successfully characterized. Investigations of impurities have included precipitates,[10–14] substitutional monovalent impurities,[15–17] and vacancy complexes.[18–19] In recent years, because of better knowledge of the lattice dynamics and also because of refined mathematical techniques, some experiments have been analyzed with the Green's-function method.[17,20–22]

The present work is a systematic study of the effect of monovalent substitutional impurities in a silver-chloride host crystal on the low-temperature thermal conductivity, supplemented by far-infrared absorptions. There have been other experiments on AgCl: Donecker[23] measured the thermal conductivity in crystals doped with Ni^{2+}, V^{2+}, Cr^{2+}, Cd^{2+}, V^{3+}, S^{2-}, Te^{2-}, Li^+, and Br^-; Bausch[24] *et al.* have observed radiation-produced colloids in AgCl. In the process of our investigation, we found that the thermal conductivity of pure or lightly doped crystals is very sensitive to the crystal handling procedures. Therefore, the pure crystals were subjected to a series of heat treatments and surface treatments to determine the effects on the conductivity. The thermal conductivity data were analyzed in the framework of the Callaway theory[25] with a modified Debye model.

II. CRYSTAL PREPARATIONS AND EXPERIMENTAL TECHNIQUES

All the pure and doped silver-chloride single crystals studied in this investigation were grown in this laboratory using the Czochralski technique. Before growth of each crystal, the reagent-grade silver-chloride powder was purified by bubbling oxygen and then chlorine through the molten salt, which was then placed under vacuum. Finally, the molten salt was passed through a capillary tube after which it solidified in a quartz crucible.[26] Pure crystals were analyzed semiquantitatively with the atomic emission spectrographic tech-

† Work supported in part by the Advanced Research Projects Agency under Contract No. SD-131.
* Present address: Illinois Institute of Technology, Department of Physics, Chicago, Ill. 60616.

[1] H. B. G. Casimir, Physica **5**, 495 (1938).
[2] R. Berman, E. L. Foster, and J. Ziman, Proc. Roy. Soc. (London) **A231**, 130 (1955).
[3] P. S. Thatcher, Phys. Rev. **156**, 965 (1967).
[4] T. H. Geballe and G. W. Hull, Phys. Rev. **110**, 773 (1958).
[5] R. Berman and J. C. Brock, Proc. Roy. Soc. (London) **A289**, 46 (1965).
[6] R. Berman, C. L. Bounds, and J. S. Rogers, Proc. Roy. Soc. (London) **A289**, 66 (1965).
[7] R. L. Sproull, M. Moss, and H. Weinstock, J. Appl. Phys. **30**, 334 (1959).
[8] A. Taylor, H. R. Albers, and R. O. Pohl, J. Appl. Phys. **36**, 2270 (1965).
[9] M. Moss, J. Appl. Phys. **36**, 3308 (1965).
[10] G. A. Slack, Phys. Rev. **105**, 832 (1957).
[11] M. V. Klein, Phys. Rev. **123**, 1977 (1961).
[12] J. W. Schwartz and C. T. Walker, Phys. Rev. **155**, 969 (1967).
[13] C. T. Walker and R. O. Pohl, Phys. Rev. **131**, 1433 (1963).
[14] J. M. Worlock, Phys. Rev. **147**, 636 (1966).
[15] F. C. Baumann, J. P. Harrison, W. D. Seward, and R. O. Pohl, Phys. Rev. **159**, 691 (1967).
[16] F. C. Baumann and R. O. Pohl, Phys. Rev. **163**, 843 (1967).
[17] R. F. Caldwell and M. V. Klein, Phys. Rev. **158**, 85 (1967).
[18] L. G. Radosevich and C. T. Walker, Phys. Rev. **156**, 85 (1967).
[19] J. W. Schwartz and C. T. Walker, Phys. Rev. **155**, 959 (1967).
[20] L. G. Radosevich and C. T. Walker, Phys. Rev. **171**, 1004 (1968).
[21] J. A. Krumhansl, in *Proceedings of International Conference on Lattice Dynamics, Copenhagen, 1963*, edited by R. F. Wallis (Pergamon Press, Ltd., Oxford, England, 1965), p. 523.
[22] C. W. McCombie and J. Slater, Proc. Phys. Soc. (London) **84**, 499 (1964).
[23] J. Donecker, Phys. Status Solidi **26**, K131 (1968).
[24] W. Bausch, F. Guckenbiehl, and W. Waidelich, Phys. Letters **28A**, 38 (1968).
[25] J. Callaway, Phys. Rev. **113**, 1046 (1959).
[26] C. Berry, W. West, and F. Moser, in *The Art and Science of Growing Crystals*, edited by J. J. Gilman (John Wiley & Sons, Inc., New York, 1963), p. 214.

nique by Mossotti and his staff at the Spectrochemical Analysis Laboratory. The results showed that a number of impurities were present in the crystals with concentrations below 10 ppm. Exceptions were magnesium and silicon which were present at the 20 ppm level. More details on crystal purification and growth technique are given elsewhere.[27]

Thermal conductivity samples were rectangular bars, about 5 mm×5 mm×40 mm and oriented along the [100] direction. The samples were polished on No. 500-grit emery paper to remove the surface damage and then etched in $3N$ $Na_2S_2O_3$ solution for one minute and rinsed with deionized water. After the etching, some crystals revealed two or three large grains within the sample. The reference pure crystal and all doped crystals were annealed at 400°C in an argon atmosphere for 10 h and then cooled at the rate of 20°C/h. Before each measurement, the sample was sandblasted to ensure diffuse boundary scattering.

The surfaces of infrared samples were polished on No. 600-grit emery paper with deionized water as a lubricant and then further polished on a soft polishing cloth which had been moistened with a 5%-KCN solution. The thermal conductivity of the pure and doped silver-chloride crystals was measured as a function of temperature from 1.2 to 80°K. The cryostat, electronics, and measuring techniques are described by Klein and Caldwell.[28]

Because of the chemical reactions of silver chloride with most metals, all metallic contacts were either silver plated or covered with gold foil. The germanium thermometer clamps are similar to those described by Klein and Caldwell, but with the indium knife edges replaced by silver-plated copper knife edges. Silver chloride is a soft material, so that in the process of mounting the thermometer clamps, the knife edges immediately deformed the crystal. As a result, the phosphor-bronze strip lost its spring action. In order to secure the clamps on the crystal, further tightening was necessary. It was found that a piece of 5-mil gold foil at the knife edge provided excellent thermal contact at all times. Unfortunately, the clamps left four grooves of 0.75-mm width and about 0.5-mm depth on the surfaces of the crystal. These deformations produced dislocations in the crystal and interfered with the phonon scattering due to the substitutional impurities.

The far-infrared absorption of pure and doped AgCl crystals was measured as a function of wave number from 33 to 105 cm^{-1} at 7°K on a Beckman IR11 spectrophotometer using a beam condenser described in detail by Brandt.[29]

[27] C. K. Chau, Ph.D. thesis, University of Illinois, 1968 (unpublished).
[28] M. V. Klein and R. F. Caldwell, Rev. Sci. Instr. **37**, 1291 (1966).
[29] R. C. Brandt, Appl. Opt. **8**, 315 (1969).

III. THERMAL CONDUCTIVITY RESULTS

A. Pure Crystals

1. Polycrystal

The low-temperature thermal conductivity of sintered alumina is dominated by crystallite boundary scattering with a phonon mean free path similar to the average grain size. This result has been clearly demonstrated by Berman.[30] We have seen a similar effect in AgCl.

The thermal conductivity of a Harshaw rolled optical sample before and after annealing is shown in Fig. 1. Bellow the maximum, the conductivity of the unannealed sample is depressed by a factor of 70 with respect to the single-crystal data. The slope is approximately 2.5. This large depression is perhaps due to crystallite

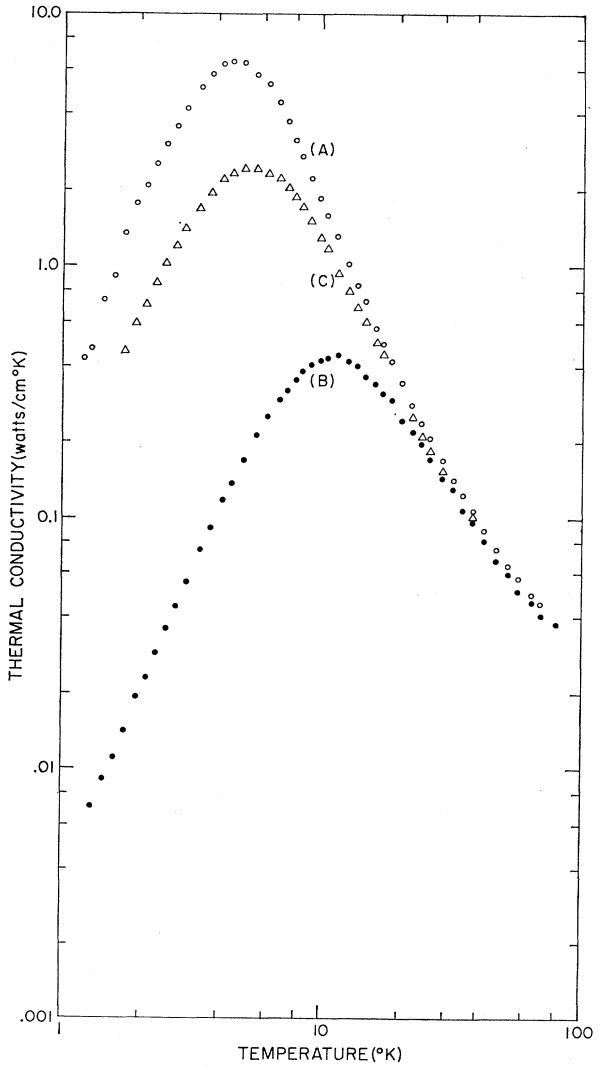

FIG. 1. Thermal conductivity data for the polycrystal. Curve *A*, pure single crystal; curve *B*, unannealed Harshaw rolled optical crystal; curve *C*, after anneal.

[30] R. Berman, Proc. Phys. Soc. (London) **A65**, 1029 (1952).

boundary scattering which limits the phonon mean free path. From the conductivity at 1.5°K, the estimated mean free path should be of the order of 60 μ. Photomicrographs reveal the average grain size to be about 5 μ. The difference between the estimated mean free path and the average grain size, and the $T^{2.5}$ dependence suggest that some specular reflection within the grains or transmission through the grain boundaries occurs. Thus, as for the sintered alumina case, diffuse crystallite boundary scattering seems very likely.

The polycrystalline sample was annealed in an argon atmosphere at 400°C for 10 h and then cooled at the rate of 25°/h. The conductivity increased by a factor of 30 and exhibited a T^2 temperature dependence. Annealing enlarges the grain size and removes strains from the crystal. The result is that the mean free path and hence the conductivity increases. The remaining depression with respect to the single-crystal curve is thought to be due to some dislocations and grain boundaries remaining in the crystal.

2. *Surface Treatments on Single Crystal*

Worlock suggested that diffuse boundary scattering is mainly due to the tangle of dislocation loops produced by sandblasting and not merely due to the irregularity of the surface.[14] We performed an experiment on a pure AgCl single crystal to confirm Worlock's suggestion. Unfortunately, we were unable to observe dislocation loops directly with Mitchell's etching procedures.[31]

Figure 2 shows a sequence of five thermal conductivity measurements on a pure AgCl single crystal (*SH*12-1-*D*-3) after it had undergone different surface treatments. The surfaces of the crystal were first ground with 2/*F* Carborundum until they were dull; then the crystal was annealed at 400°C for 10 h and cooled at the rate of 20°C/h. Its conductivity is shown in curve *A*. After the first measurement, the crystal was gently polished with Kimwipes disposable wipers until the surfaces were reflective. The conductivity was depressed below the maximum as shown in curve *B*. This indicates that an additional scattering mechanism was introduced during the polishing. The crystal was then reannealed in the previous manner and then etched in 5%-KCN solution for 2 min; the final surfaces were fairly smooth and highly reflective. The resulting conductivity curve *C* increased above curve *A*. This indicated that some scattering mechanism present for curves *A* and *B* was partially or completely removed from the crystal. For curve *D*, the crystal surfaces were ground again with No. 500 grit emery paper. The conductivity curve depressed and fell slightly below curve *B*. This shows that some scattering mechanism was introduced with strength similar to that in stage *B*. Finally, for curve *E*, the crystal was irradiated with 3-MeV γ rays. The γ-ray source was a gold target bombarded by a high-energy electron beam from the Van de Graaff accelerator in the Materials Research Laboratory. The estimated number of charged particles produced in the crystal was approximately 10^7 esu/cc. The conductivity curve *E* increased, indicating that γ radiation lessens the effect of the defects in stage *D* and reduces the total scattering strength.

With a modification of Worlock's suggestion, it is possible to explain the results of each surface treatment. Assume that the important ingredient needed to achieve diffuse boundary scattering in AgCl is the presence of dynamical dislocation loops just beneath the surface of the crystal. They can be generated by rubbing the crystal surface. For curve *A*, the dynamical dislocations generated in the process of grinding were removed by the careful annealing. The boundary scattering is due only to the rough surfaces and is partly diffuse and partly specular. For curve *B*, the dislocation loops were introduced and reduced the degree of specular boundary scattering thus lowering the conductivity. For curve *C*, we purposely remove the dislocation loops and rough surfaces by annealing and etching. Now the boundary scattering is mainly specular, hence the highest conductivity is achieved. For curve *D*, dislocation loops were reintroduced into the crystal, but the surfaces were less irregular than for curve *A*. As a result, the conductivity is again depressed and is similar to stage *B*. This suggests that the main mechanism for diffuse boundary scattering is dynamical dislocation loops just beneath the surfaces but not the irregularity of the surface. If this interpretation is correct, then one can pin down these dynamical dislocation loops by means of γ irradiation. This was performed for curve *E*, and the result shows the conductivity increase after the irradiation. We may conclude that dynamical dislocation loops scatter phonons very effectively and can be generated just beneath the surface by gentle rubbing. However, during this sequence of treatments, the crystal was handled extensively. It is also not clear whether there are any other defects being introduced. In future work, it may be desirable to repeat stages *D* and *E* and perform the irradiation with the crystal mounted in the cryostat, at liquid-nitrogen temperature.

3. *Heat Treatments on Single Crystals*

Heat treatments were performed on two pure AgCl crystals (*SH*12-1-*D*-2, *SH*12-1-*D*-3) which were cut from the same bulk material adjacent to each other. Prior to the cooling of each crystal, the specimens had been annealed at 400°C for 10 h. They also had identical surface preparations, and thus the observed effects are solely bulk effects. The results for each heat treatment are shown in Fig. 3.

Curve *A* shows crystal *SH*12-1-*D*-2 which was cooled at a rate of 20°C/h. It gives the highest thermal conductivity. Curve *B* shows the same sample cooled

[31] J. W. Mitchell, in *Dislocation and Mechanical Properties of Crystals*, edited by J. C. Fisher, W. B. Johnston, R. Thomson, and T. Vreeland (John Wiley & Sons, Inc., New York, 1957), p. 69.

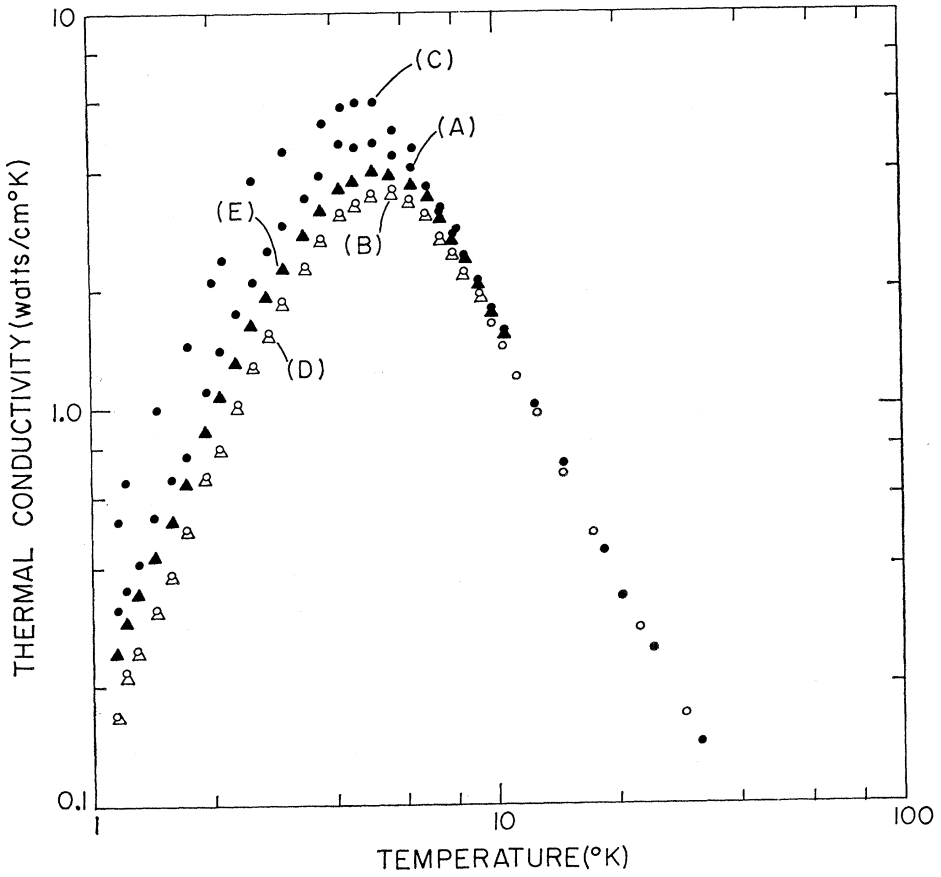

FIG. 2. Thermal conductivity data for the surface treatments on the single crystal. Curve *A*, ground surface; curve *B*, polished surface; curve *C*, reannealed and etched surface; curve *D*, reground surface; curve *E*, irradiated.

at 40°C/h. The conductivity below the maximum is depressed and the slope is 2.5. Crystal *SH*12-1-*D*-3 was quenched to room temperature in less than 20 min. Its conductivity, which is similar to curve *B*, is given by curve *C*. Curve *D* shows the same crystal quenched to liquid-nitrogen temperature and then brought back to room temperature before mounting in the cryostat. There is no pronounced effect on the thermal conductivity.

Two possible phonon scattering mechanisms may arise during the rapid cooling or quenching of the single crystals. We point out that Castle observed the dislocation density in a well-annealed silver-chloride crystal[32] to be about $10^5/cm^2$. We expect this density to have essentially no effect on the thermal conductivity. Rapid cooling and quenching, however, exert thermal stress on the crystal; hence fresh dislocations may be formed in the process. From the degree of low-temperature depression, we may estimate the dislocation density to be about $10^7/cm^2$ according to Ohashi's theory[33] which is discussed in Sec. VI. This is well within the limits of 10^6–$10^8/cm^2$ observed in crystals which had been annealed at 400°C and then deformed.[31]

Second, in ionic crystals an edge dislocation is electrostatically charged, and in thermodynamic equilibrium its core is necessarily surrounded by charge-compensating clouds.[34,35] Plint and Breig[36] used a light scattering method to demonstrate the presence of long-cylindrical scattering centers in the crystals. These were presumably charge clouds surrounding dislocations. With 10–20 ppm of divalent impurities in our samples and an annealing time of 10 h at 400°C, one might expect the impurities along with vacancies and interstitials to establish equilibrium by forming charge clouds around dislocations. By rapid cooling or quenching one might expect the charge cloud to remain in frozen metastable equilibrium. Then phonons will be scattered by cylinders with an effective size similar to the Debye-Hückel radius instead of bare dislocations. The relaxation rate for phonon scattering by a cylinder perpendicular to temperature gradient is given by Klemens[37]; it is proportional to the fourth power of the radius of the cylinder and to the third

[32] J. Castle, J. Appl. Phys. **28**, 742 (1957).
[33] K. Ohashi, J. Phys. Soc. Japan **24**, 437 (1968).
[34] J. S. Koehler, D. Langreth, and B. von Turkovich, Phys. Rev. **128**, 573 (1962).
[35] A. Hikata, C. Elbaum, B. Chick, and R. Truell, J. Appl. Phys. **34**, 2154 (1963).
[36] C. Plint and M. Breig, J. Appl. Phys. **35**, 2745 (1964).
[37] P. G. Klemens, in *Solid State Physics*, edited by F. Seitz and D. Turnbull (Academic Press Inc., New York, 1958), Vol. 7.

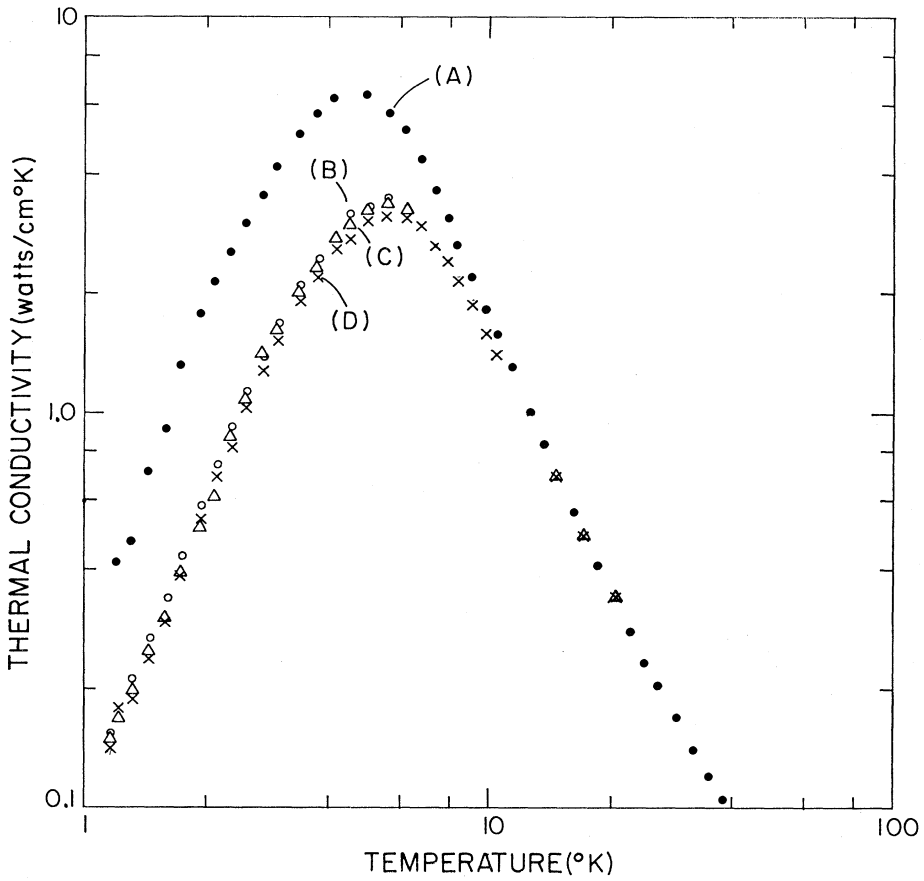

FIG. 3. Thermal conductivity data for the heat treatments on the single crystals. The single crystals were annealed at 400°C for 10 h and cooled at the following rates: Curve *A* 20°C/h; curve *B* 40°C/h; curve *C* quenched to room temperature in less than 20 min; curve *D* quenched to liquid-nitrogen temperature.

power of the frequency. Therefore, the choice of radius is very important in determining the strength of the scattering. The Debye-Hückel radius is determined by the temperature at equilibrium.

It must be pointed out, however, that our assumption of charge clouds which freeze immediately is not strictly correct. The reason is that the divalent impurity ions and silver-ion interstitials and vacancies remain mobile well below 400°C. The final configuration of the charge cloud must be determined by considering each freezing stage. If the dominating process is the scattering by cylinders, then curves *B*, *C*, *D* show a similar charge cloud radius for all three cases. We also note that pure charge-cloud scattering will not give the observed $T^{2.5}$ dependence, and other scattering processes must occur. The relative importance of these two-phonon scattering processes could be assessed by performing two consecutive measurements: first measure a quenched crystal, then remeasure the same crystal after it is deformed at liquid-nitrogen temperature. In the latter case, the freshly created dislocations would certainly be bare.

B. Doped Crystals

Figures 4–9 show the thermal conductivity data for the Li^+-, Na^+-, K^+-, Rb^+-, Br^--, and I^--doped crystals. Each figure shows the data of the reference pure crystal and the doped crystal in various concentrations, which are summarized in Table III below. Because of the limited solubility of each impurity in silver chloride, the above data are from samples without noticeable precipitations. In addition, theoretical curves are plotted for comparison. These are discussed below.

IV. FAR-INFRARED ABSORPTION RESULTS

A. Pure Crystal

The purpose of this measurement was to search for isotope-induced absorptions such as were found in alkali halides[38] and any absorptions induced by the background impurities. The optical density of a 1.25-mm-thick pure crystal, curve *D* in Fig. 10, shows that the absorption increases toward the reststrahl frequency and no peaks are observed.

B. Doped Crystals

Three concentrations of NaCl-doped crystals have been measured in the same way as the pure crystal. Their optical densities are shown in curves *A*, *B*, and

[38] M. V. Klein and H. F. Macdonald, Phys. Rev. Letters **20**, 1031 (1968).

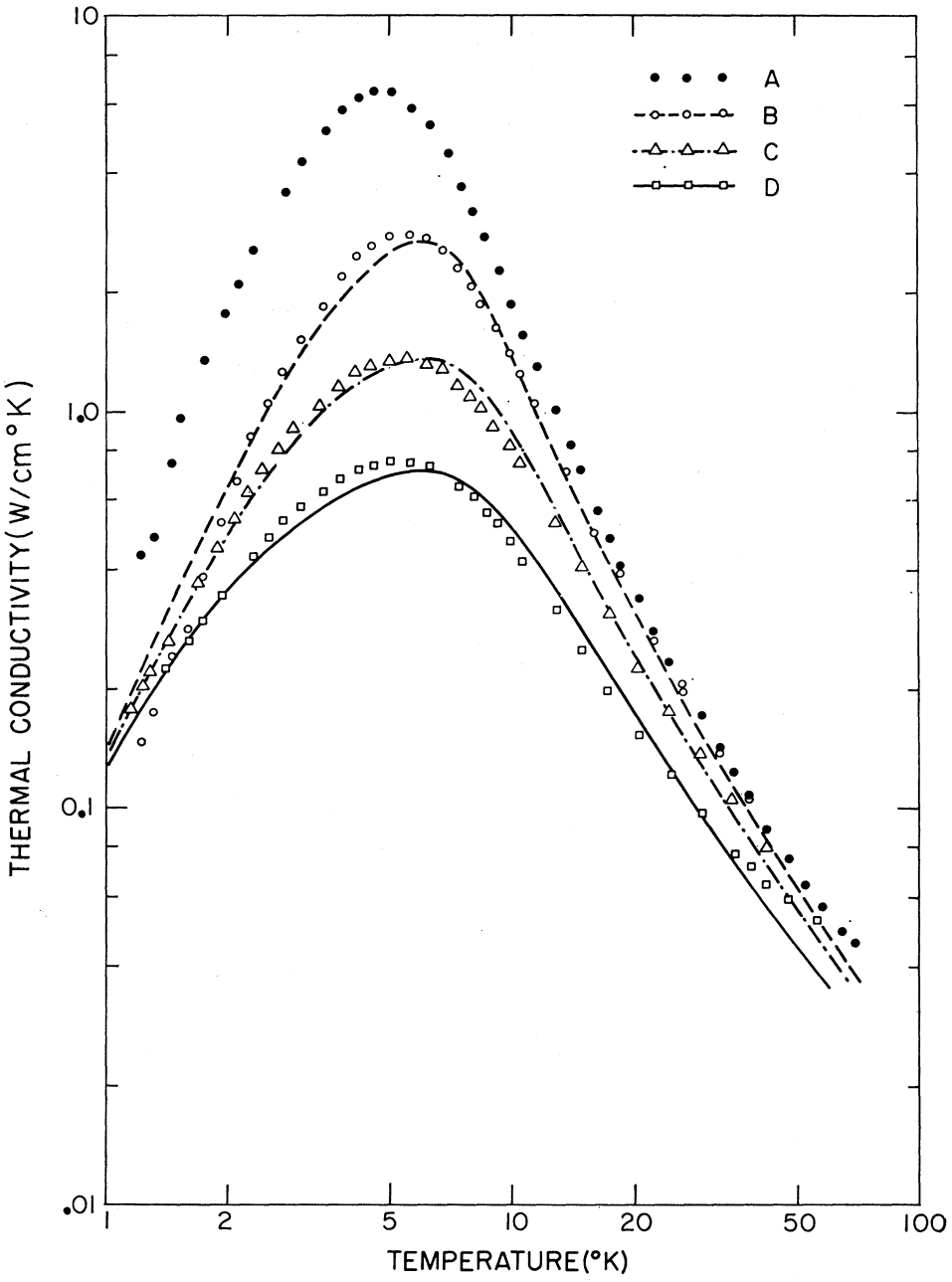

FIG. 4. Theoretical fit and thermal conductivity data for the system AgCl:LiCl. Curve *A*, pure; curve *B*, 0.017 mole%; curve *C*, 0.29 mole%; curve *D*, 0.67 mole%.

C in Fig. 10. A measurement was also performed on one sample of each of the other impurity-doped crystals. Absorption peaks were found in each doped crystal except for rubidium. This is perhaps due to the low concentration of rubidium in the crystal. These impurity doped crystals were measured against a pure crystal of the same thickness. The mismatch of the thickness was less than 5%. The impurity-induced optical densities of the Li^+-, Cu^+-, and K^+-doped crystals are curves *A*, *B*, and *C* in Fig. 11, respectively. The impurity-induced optical densities of I^-- and Br^--doped crystals are the curves *A* and *B* in Fig. 12. All impurity induced absorption peaks and sample thicknesses are summarized in Table I.

V. ANALYSIS

An expression that is often used for the lattice thermal conductivity is

$$K=\frac{\hbar^2}{3K_BT^2}\int_0^{\omega_m} d\omega\,\tau_c v^2(\omega)\rho(\omega)\frac{e^x}{(e^x-1)^2}, \qquad (1)$$

where K_B is the Boltzmann constant, v is the average group velocity for states with phonon energy $\hbar\omega$, $\rho(\omega)$

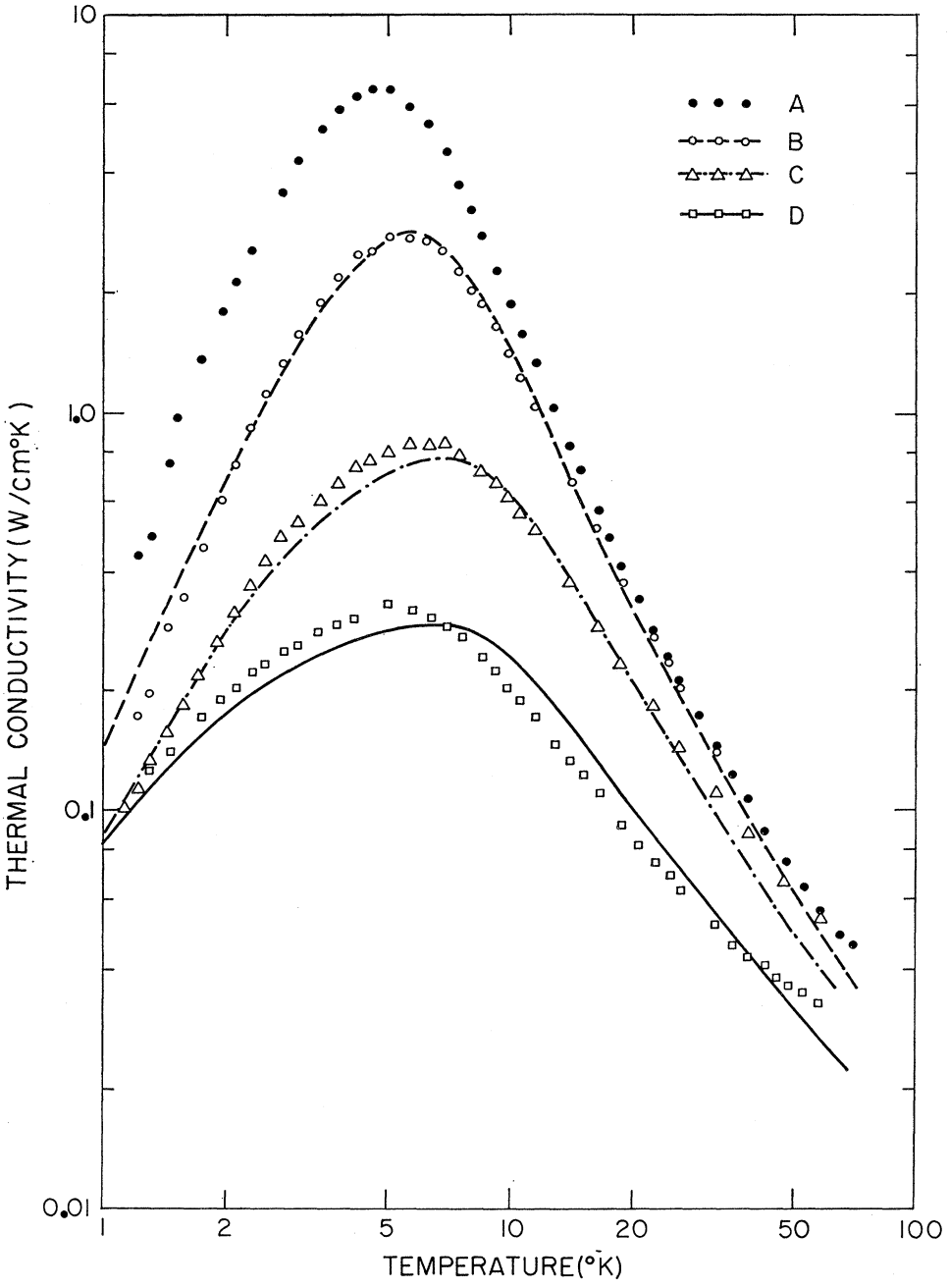

FIG. 5. Theoretical fit and thermal conductivity data for the system AgCl:NaCl. Curve *A*, pure; curve *B*, 0.048 mole%; curve *C*, 0.59 mole%; curve *D*, 4.16 mole%.

is the density of states, x is defined as $\hbar\omega/K_BT$, ω_m is the maximum allowed frequency, and τ_c is the over-all relaxation time due to several phonon scattering process. Under the Debye approximation, a crystal lattice is assumed to be isotropic and there is no dispersion in the frequency–versus–wave-vector relation. All phonons in the lattice have the same group velocity, which is also identical to the phase velocity. Use of the Debye approximation in Eq. (1) has been quite successful with many alkali-halide crystals. We can see why by making a comparison of a simple Debye model and a shell model, which represents phonons more realistically. We consider the sodium-chloride crystal for which shell-model phonons have been calculated by Caldwell and Klein.[17]

The first critical point of NaCl occurs at 80 cm^{-1} corresponding to a temperature of 115°K. The Debye density of states is in good agreement with the true density of states calculated from the shell model in this frequency range. The average group velocity as a function of frequency, calculated according to the shell model, is constant at low frequency and then decreases

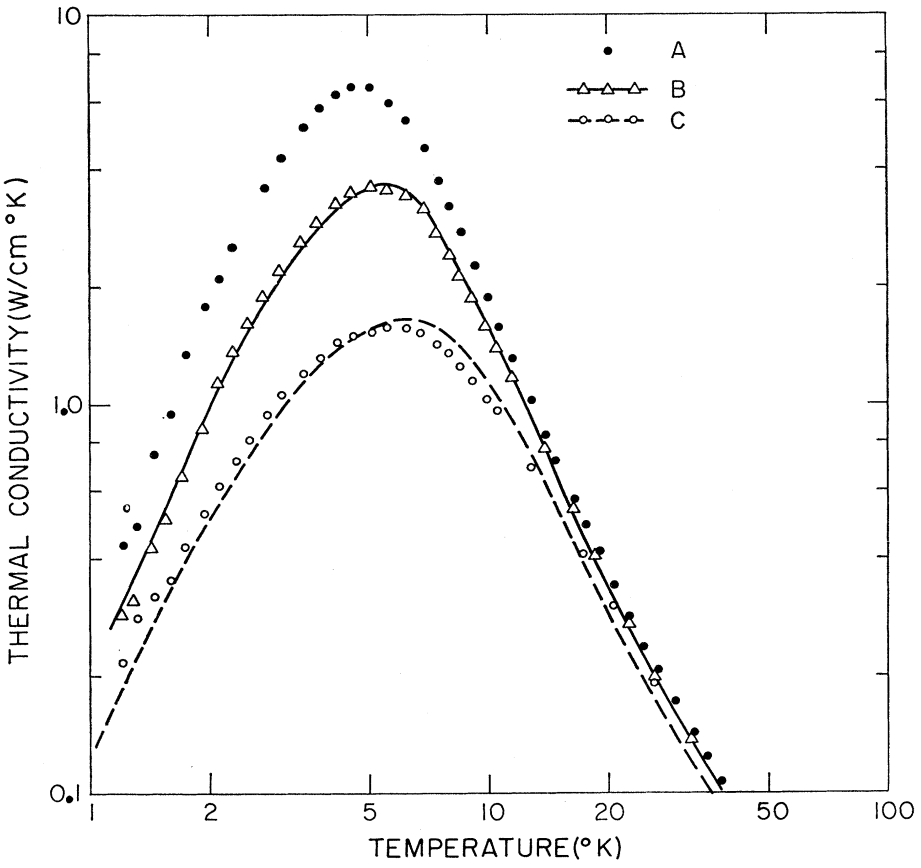

FIG. 6. Theoretical fit and thermal conductivity data for the system AgCl:KCl. Curve *A*, pure; curve *B*, 0.035 mole%; curve *C*; 0.037 mole% (see Table III, footnote f).

rapidly when approaching the first critical point. The average group velocity further decreases when passing through the other critical points and finally recovers in the region of the optical branches.

The thermal conductivity integrand without the total relaxation rate is

$$v^2(\omega)\rho(\omega)\omega^2[e^x/(e^x-1)^2]. \quad (2)$$

This quantity calculated with the shell model and the Debye model is shown in Fig. 13. The average group velocity for the Debye model is 3.84×10^5 cm/sec, corresponding to the Debye temperature of 326°C for NaCl.[39] The agreement between the two models is quite good for the low-frequency region (below 110 cm^{-1}) even at high temperatures. The deviation becomes important in the high-frequency region (above 110 cm^{-1}), where there are many critical points. Here the Debye model overestimates the high-frequency phonon contributions to the NaCl thermal conductivity calculation at temperatures above 30°K.

Recently, Nicklow and Vijayaraghaven have measured the dispersion curves of AgCl using neutron

TABLE I. Summary of impurity-induced infrared absorption peaks.

Figure	Curve	Dopant	Thickness (mm)	Position of peak in cm^{-1} (peak absorption constant in cm^{-1})
10	*A*	Na^+	1.025	70±3(23.9), 50±1.5(5.29)
10	*B*	Na^+	0.76	70±3(8.60), 50±1.5(2.54)
10	*C*	Na^+	1.26	70±3(1.61), 50±1.5 (0.58)
11	*A*	Li^+	1.25	95±2(17.3), 69±3(2.58)
11	*B*	Cu^+	1.26	98±2(5.5), 98±2(4.24), 60±2(0.116) 48±1.5(2.56), 76±3(2.77)
11	*C*	K^+	1.26	83±2(1.85)
12	*A*	I^-	1.30	86±2(2.94), 64±2(1.52)
12	*B*	Br^-	1.29	81±2(2.95), 64±2 (0.461)

[39] G. Leibfried and W. Ludwig, in *Solid State Physics*, edited by F. Seitz and D. Turnbull (Academic Press Inc., New York, 1961), Vol. 12.

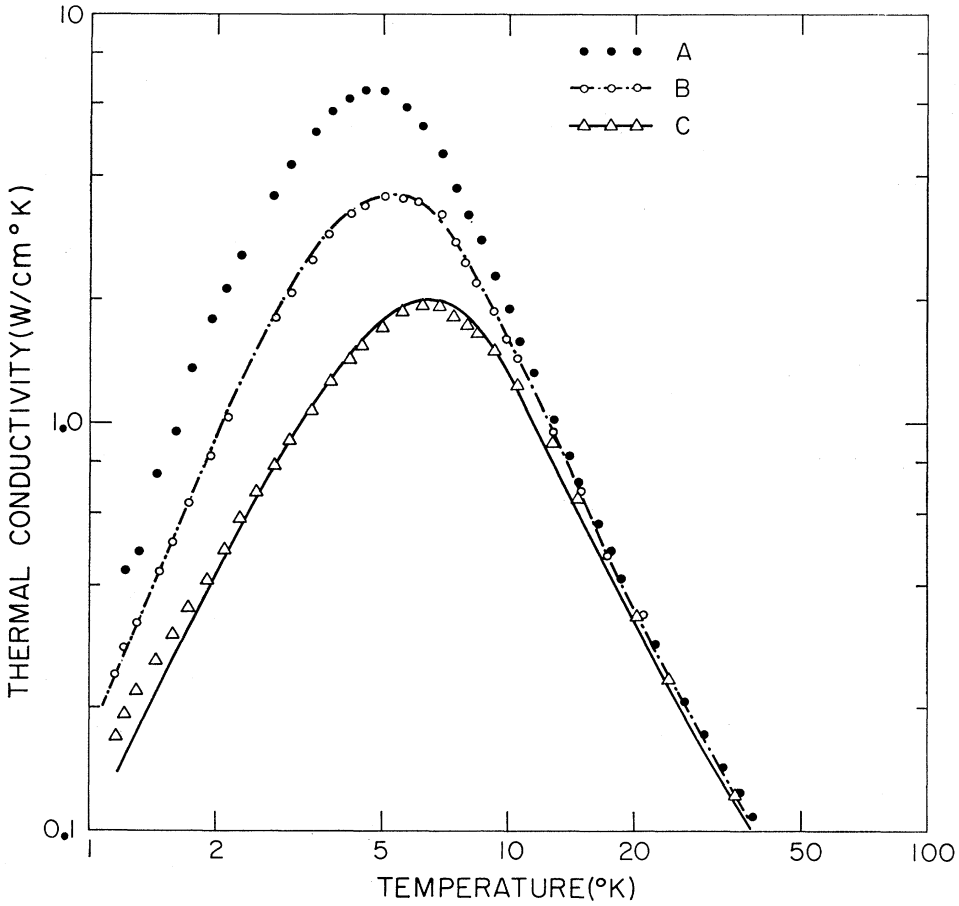

FIG. 7. Theoretical fit and thermal conductivity data for the system AgCl:RbCl. Curve *A*, pure; curve *B*, 0.0011 mole%; curve *C*, 0.024 mole%.

diffraction techniques at liquid-nitrogen temperature.[40] Their results show many critical points in the frequency region corresponding to the temperatures above the thermal conductivity maximum. These critical points are summarized in Table II along with Cole's room-temperature x-ray data.[41] The phonon states at the critical points will not contribute to thermal conduction because they have zero group velocity. This, rather than a strong umklapp process, is perhaps the true explanation of the rapid decrease of the thermal conductivity above the maximum. The conductivity integrand for silver chloride probably has the same general structure as for sodium chloride but with the high-frequency deviations shifted to lower frequencies. Hence, the Debye model not only overestimates the integrand at moderately high temperatures but also at lower temperatures. A more refined model is needed for the theoretical calculation of the thermal conductivity of silver chloride. Details of unsuccessful curve fitting with the simple Debye model are given elsewhere.[27]

TABLE II. Summary of critical points in silver chloride.

Branch and direction	Neutron data[a] (cm^{-1})	X-ray data[b] (cm^{-1})
TA[100]	33.3 ZB[c]	30
LA[100]	54.0 ZB	60
TA[110]	53.3	TA_2 33.3
		TA_1 50.0
LA[110]	38.3	66.6
TA[111]	71.6 ZB	40
TO[111]	76.6 ZB	66.0
LA[111]	100 ZB	
TO[100]	150 ZB	
LO[100]	200 ZB	
LO[111]	203 ZB	
LO[110]	196.6 ZB	
TO[110]	163.3 ZB	
TO	121.6 C[d]	
LO	193.3 C	

[a] Neutron diffraction data was obtained at liquid-nitrogen temperature by Nicklow and Vijayaraghavan (Ref. 40).
[b] X-ray diffusive scattering data from Cole (Ref. 41).
[c] ZB: Zone boundary.
[d] C: Center of the zone.

A. Two-Group-Velocity and Multiple-Group-Velocity Models

We now propose a simple two-group-velocity model. It considers the lattice to be isotropic, but the frequency–versus–wave-vector relation is altered. The

[40] R. M. Nicklow and P. R. Vijayaraghavan, Bull. Am. Phys. 14, 302 (1969); and private communication.

[41] H. Cole, J. Appl. Phys. 24, 482 (1953).

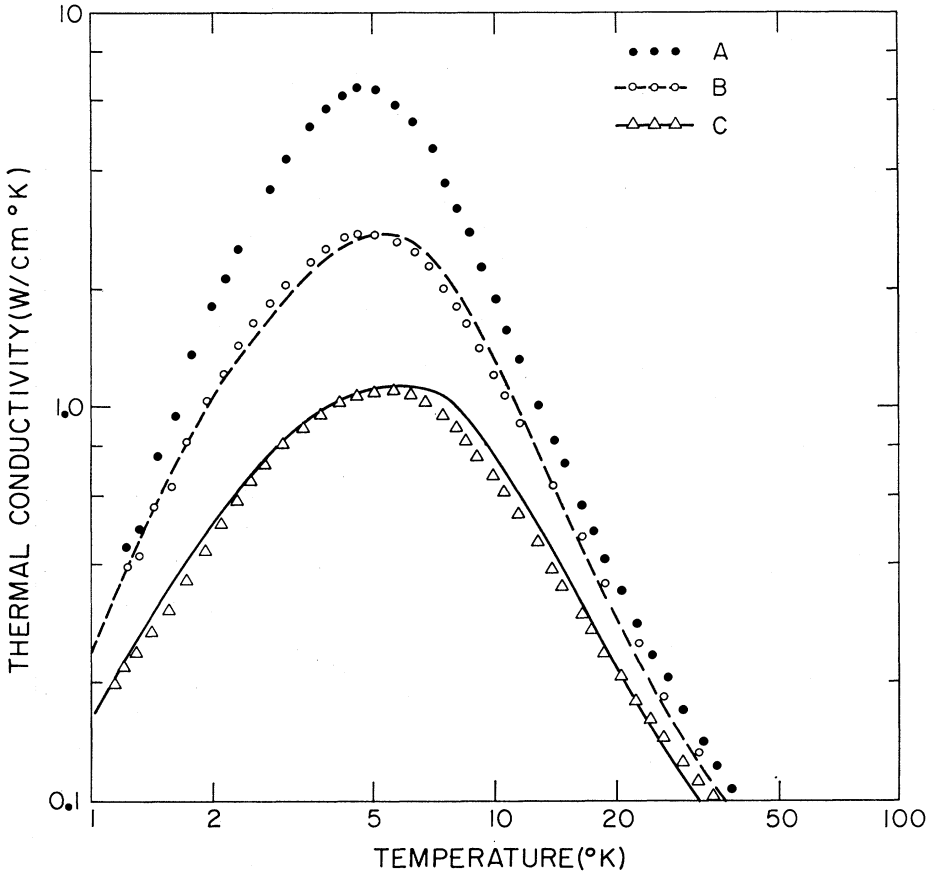

FIG. 8. Theoretical fit and thermal conductivity data for the system AgCl:AgBr. Curve *A*, pure; curve *B*, 0.13 mole%; curve *C*, 1.7 mole%.

group velocity v_1 is assumed constant up to a certain critical frequency ω_1; then it is changed to another constant value v_2. The phase and group velocities of phonons above the critical frequency will be different. Below ω_1, the phase velocity and group velocity are

$$v_p=v_1 \quad \text{and} \quad v_g=v_1. \tag{3}$$

Above the critical frequency ω_1,

$$v_p=v_2\frac{\omega}{\omega-\omega_1(1-v_2/v_1)} \quad \text{and} \quad v_g=v_2. \tag{4a}$$

The total number of phonon states is restricted by the number of molecules in the crystal. Therefore, the total number of states must be conserved regardless of the model that we use. In the Debye model, the Debye temperature corresponds to a maximum frequency with the property that the total number of states below this frequency is equal to the total number of degrees of freedom in the crystal. We also have to restrict the total number of states in the two-group-velocity model by use of a certain maximum frequency. If v_2 is less than v_1, the maximum frequency is lower than that in the simple Debye model. This is favorable to our case since it suppresses the high-frequency phonons.

This modified Debye model introduces two extra parameters into the calculation; the critical frequency ω_1 and the second group velocity v_2. With this model, a step occurs in the density-of-states and the thermal conductivity integrand curves due to the discontinuity of the group velocity at ω_1. This step can be removed with a further refinement: The multiple-group-velocity model. In this refined model, the group velocity gradually changes from v_1 to v_2. This transitional region can be described by using a Fermi-Dirac function, and the rate of transition is governed by a width parameter D.

B. Two-Group-Velocity Model Fits

We choose the two-group-velocity model over the multiple-group-velocity model to avoid the addition of the width parameter D. With this model, the conductivity integral has to be modified to account for the variation of the group velocity and phase velocity. It must be written explicitly in terms of v_g and v_p,

$$K=1.57\times10^9T^3\int_0^{x_m}\tau_c(v_g,v_p,x,T)\frac{Q^2}{v_g}\frac{e^x x^4}{(e^x-1)^2}dx, \tag{4b}$$

where

$$x=\hbar\omega/K_BT \tag{4c}$$

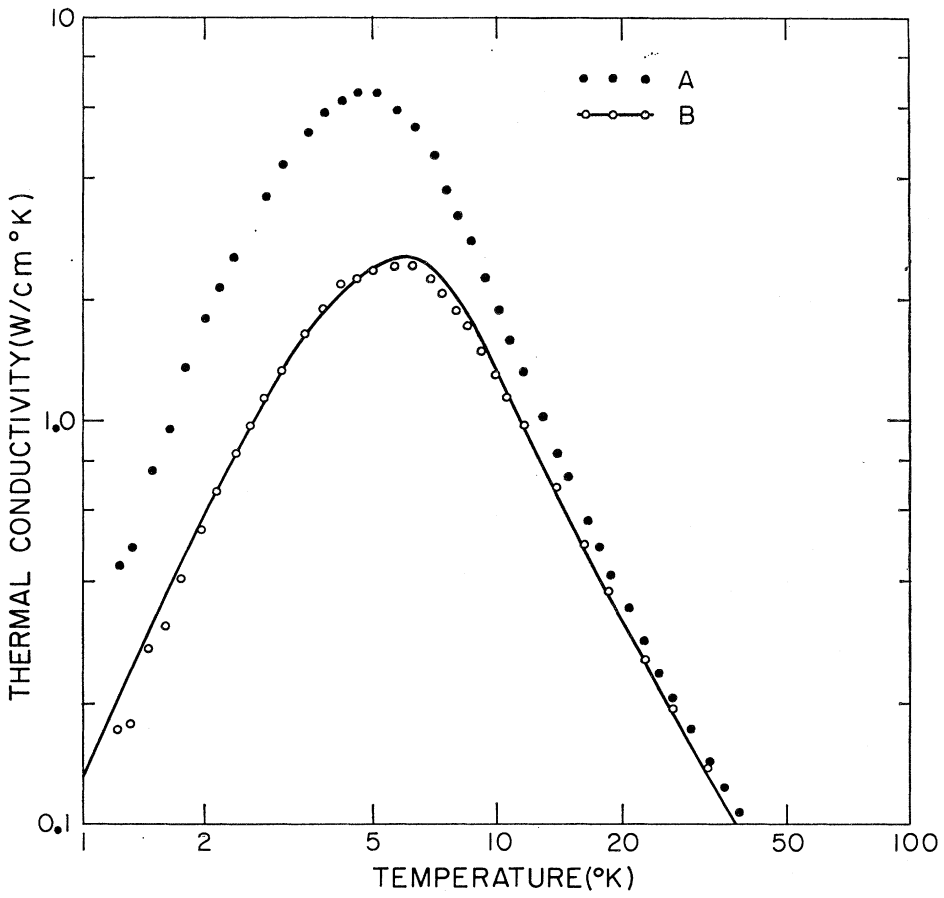

FIG. 9. Theoretical fit and thermal conductivity data for the system AgCl:AgI. Curve A, pure; curve B, 0.061 mole%

and

$$Q=v_g/v_p. \tag{4d}$$

The group velocities are obtained from the low-temperature elastic constants.[42] We use $v_1=1.62\times10^5$ cm/sec which is the rms value of the group velocities as calculated by the Houston method.[43] The critical frequency $\omega_1=31.2$ cm^{-1} (45°K), was chosen to be near the first critical point in the silver-chloride phonon spectrum. We use a value $v_2=8\times10^4$ cm/sec which is approximately half of the average group velocity in the first range and is similar to the sodium-chloride case. The maximum frequency is 57 cm^{-1} (82°K) which is obtained from the Debye temperature of 215°K as given by Nicklow and Young from specific-heat data.[44]

C. Pure Crystal Fit

An appropriate total relaxation rate includes normal and umklapp three-phonon scattering processes, boundary scattering, and isotope scattering for the pure silver-chloride crystal. The theoretical boundary-scattering relaxation rate is

$$1/\tau(\text{boundary})=Cv_g=v_g/1.12d\eta. \tag{5}$$

For our crystal $d=0.555$ cm and the finite-length correction factor η is 0.6 as given by Berman, *et al.*[2] Therefore, C is equal to 2.68. The fitted value was 5.0.

Klemens[45] has derived an expression for the scattering rate due to randomly isolated point defects:

$$1/\tau(\text{point defect})=(n\Omega_0/4\pi v^3)\omega^4S^2, \tag{6a}$$

$$S^2=(\Delta M/M)^2+2(\Delta F/F-13.44(\Delta R/R))^2, \tag{6b}$$

where Ω_0 is the unit-cell volume, n is the defect concentration, ΔM is the mass difference between host and impurity atom, ΔF is the change in the coupling constant (this is related to the compressibilities of host and impurity atoms), ΔR is the change in the nearest-neighbor distance, M is the average molecular mass, and v is the average group velocity. For isotope scattering, Eq. (6) reduces to

$$1/\tau(\text{isotope})=(\Omega_0/4\pi v^3)\omega^4S_0^2, \tag{7}$$

where

$$S_0^2=\sum_i f_i(1-M_i/M)^2,$$

[42] W. Hidshaw, J. T. Lewis, and C. V. Briscoe, Phys. Rev. **163**, 876 (1967).
[43] D. D. Betts, Z. B. Bhatis, and M. Wyman, Phys. Rev. **104**, 37 (1956).
[44] R. Nicklow and R. Young, Phys. Rev. **129**, 1936 (1963).
[45] P. G. Klemens, Proc. Roy. Soc. (London) **A68**, 113 (1955).

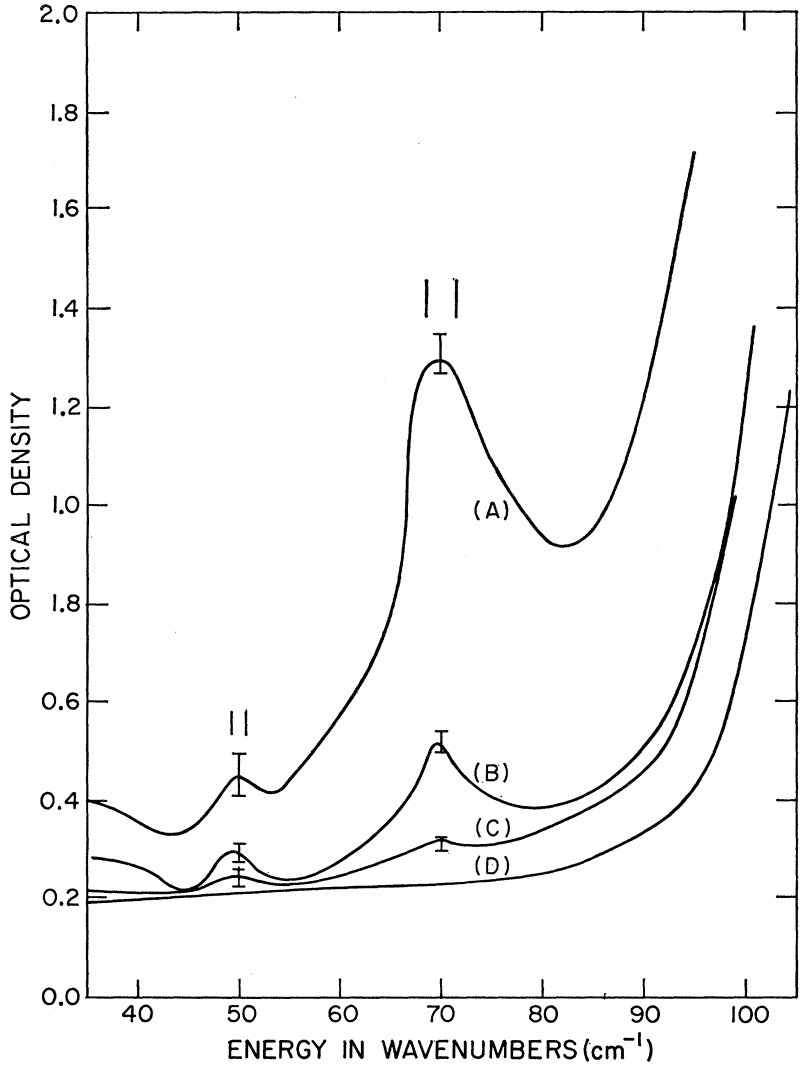

FIG. 10. Optical density of the far-infrared absorptions. Curve A, 4.16 mole% of Na^+; curve B, 0.591 mole% of Na^+; curve C, 0.0479 mole% of Na^+; curve D, pure. Crystal thickness is given in Table I.

where f_i is the fractional concentration of the ith isotope, and M_i is the mass of the ith isotope. The theoretical value of S_0^2 is 8.03×10^{-5}, in comparison with the fitted value, 9.03×10^{-5}. This large fitted value is perhaps due to other background impurities in the pure crystal that contribute to the Rayleigh scattering. The normal and umklapp three-phonon relaxation rates used for the fit are

$$1/\tau(\text{normal})=B_1\omega^2T^{2.5} \tag{8a}$$

and

$$1/\tau(\text{umklapp})=B_2\omega^2Te^{-35/T}, \tag{8b}$$

where

$$B_1=5.0\times10^{-20} \quad \text{and} \quad B_2=2.0\times10^{-17}.$$

To summarize, the total relaxation rate used to fit the thermal conductivity of the pure silver-chloride crystal is

$$\omega<\omega_1 \quad (1/\tau_c)=8.1\times10^5+7.54\times10^{-44}\omega^4 +5.0\times10^{-20}\omega^2T^{2.5}+2.03\times10^{-17}\omega^2Te^{-35/T}, \tag{9a}$$

$$\omega_m>\omega>\omega_1 \quad (1/\tau_c)=4.0\times10^5+6.25\times10^{-43}\omega^4Q^2 +5.0\times10^{-20}\omega^2T^{2.5}+2.03\times10^{-17}\omega^2Te^{-35/T}, \tag{9b}$$

where

$$Q=\frac{\omega-\omega_1(1-v_2/v_1)}{\omega}.$$

The result of the theoretical curve is shown in Fig. 14. Note the large coefficient for the normal process that is necessary to fit the pure-crystal data. This suggests that the anharmonicity in AgCl is strong, in agreement with findings of Hidshaw *et al.*[42]

D. Doped-Crystal Fit

The two important scattering processes in the doped crystals which we believe to have the strongest influence on the conductivity are simple point-defect scattering expressed in Eq. (6) and static-dislocation scattering. The dislocation-scattering relaxation rate of the form

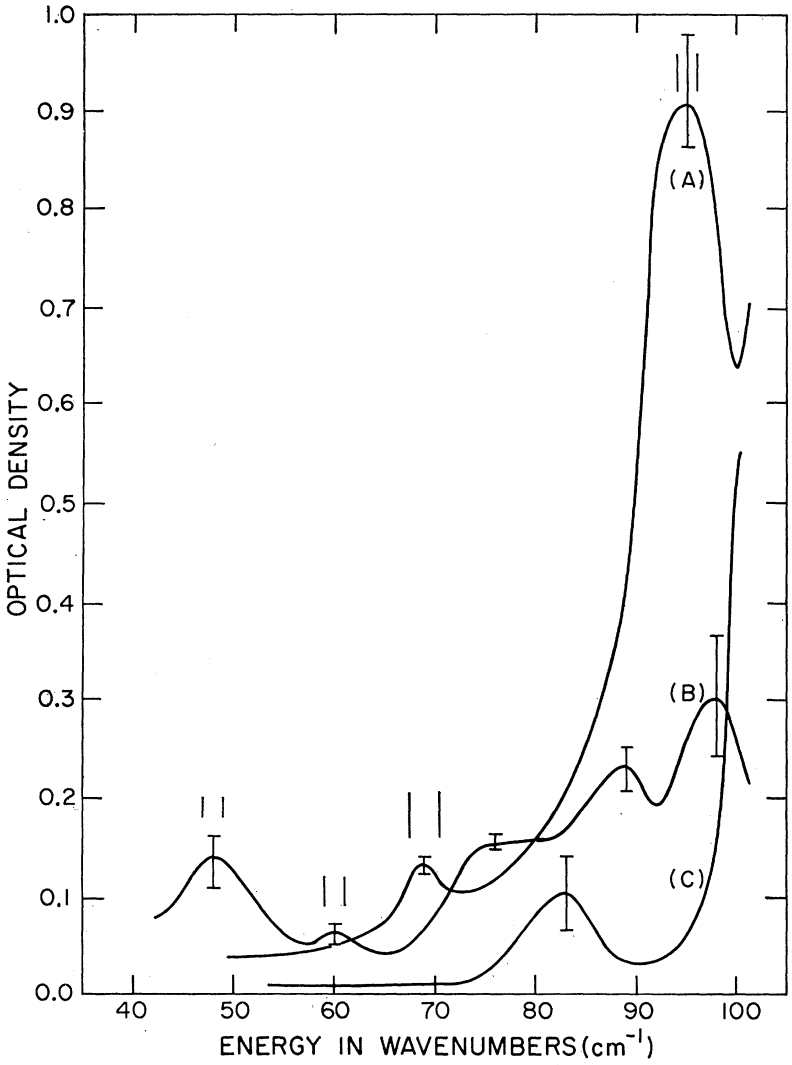

FIG. 11. Optical density of impurity-induced far-infrared absorptions. Curve A, 0.291 mole% of Li^+; curve B, 0.0654 mole% of Cu^+; curve C, 0.37 mole% of K^+. Crystal thickness is given in Table I.

derived by Klemens,[45] Carruthers,[46] and Ohashi[33] is

$$1/\tau(\text{dislocation}) = W\omega, \tag{10}$$

where $W=\rho\Gamma$, ρ is the density of dislocations, and Γ is the strength of the scattering which is different for each theory. We add these two additional relaxation rates to that of the pure crystal and then fit all the curves of the doped crystals by adjusting the quantities $Y(=NS^2)$ and W. The fitted curves for Li^+-, Na^+-, K^+-, Rb^+-, Br^--, and I^--doped crystals are shown in Figs. 4–9. The results of all fitted parameters and a comparison of their theoretical values are summarized in Table III. The quantities S^2 and all relevant constants for evaluating S^2 are given in Tables IV and V,[47–49] respectively. The conductivity curves of the copper-doped crystal have not been fitted, but they are discussed in Sec. VII.

VI. INTERPRETATIONS

A. Temperature Region above Conductivity Maximum

Our analysis shows that the point-defect scattering as described by Eq. (6) gives good agreement with the data on low-impurity-concentration crystals. For high-impurity concentrations, the conductivity curves recover from the maximum depression to approach the pure curve at a much faster rate than that caused by Rayleigh scattering. The fitted values of Y do not scale with the measured impurity concentrations (see Table III). Hence, we suggest that another scattering mechanism must occur. With far-infrared measurements on alkali halides, one may observe odd-parity impurity resonance modes in the form of peaks at energies corresponding to the resonance frequencies. In thermal

[46] P. Carruthers, Rev. Mod. Phys. **33**, 92 (1961).
[47] J. T. Lewis, A. Lehoczky, and C. V. Briscoe, Phys. Rev. **161**, 877 (1967).
[48] M. H. Norwood and C. V. Briscoe, Phys. Rev. **112**, 45 (1958).
[49] H. B. Huntington, in *Solid State Physics*, edited by F. Seitz and D. Turnbull (Academic Press Inc., New York, 1956), Vol. 7.

conductivity measurements, one may detect both odd- and even-parity impurity resonances in the form of a dip or dips at temperatures corresponding to the resonance frequencies. Therefore, impurity resonance modes which are detected in the infrared absorption may also be detected in the thermal conductivity, but the reverse situation may not be true. We should point out that the thermal conductivity is more effective in detecting a resonance with a large width, but far-infrared absorption is more effective in detecting narrow resonances.

The relation between the resonance frequency and the conductivity-dip temperature is

$$\omega_r(\mathrm{cm}^{-1}) \approx \sigma T_{\mathrm{dip}}(^\circ\mathrm{K}),$$

where ω_r is the resonance frequency, T_{dip} is the corresponding conductivity-dip temperature, and σ is the scaling factor. This scaling factor varies for different host crystals and also depends on the parity of the resonance. The value 2.66 may be obtained with the Debye model by maximizing the thermal conductivity integrand [see Eq. (2)]. This gives the predominant phonons in the lattice at a given temperature. The resonance relaxation rates derived by Klein[50] have frequency dependences which tend to shift the scaling factors to smaller values. This effect is observed in different ionic crystals where the scaling factors range from 1.2 to 2.6. A detailed study of the relation of the conductivity dip to the resonance frequency within the Debye model has been carried out by Rosenbaum.[51]

It may be difficult to relate the far-infrared absorption to the thermal conductivity in weakly perturbed systems. The presence of impurities will destroy the translational system of the perfect lattice, hence the wave-vector selection rules will be relaxed, and acoustic modes of lattice vibration can be excited by the far-infrared radiation. Then the absorption peaks may

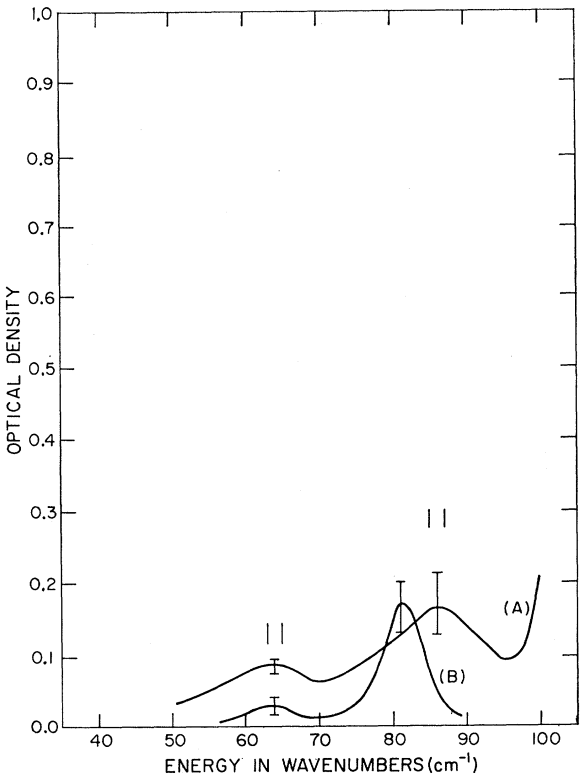

FIG. 12. Optical density of impurity-induced far-infrared absorptions. Curve A, 0.29 mole% of I^-; curve B, 0.13 mole% of Br^-. Crystal thickness is given in Table I.

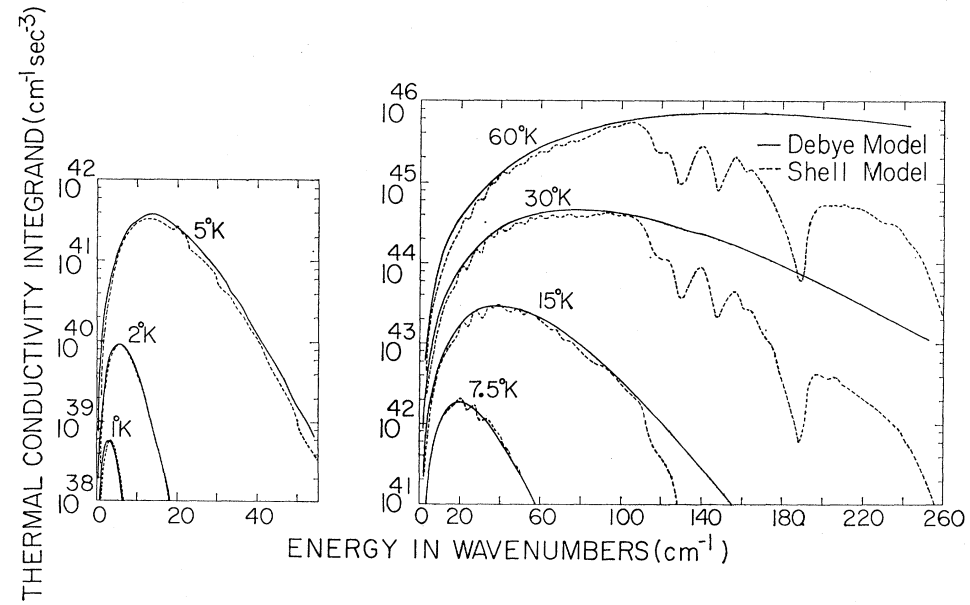

FIG. 13. Comparison of Debye-model and shell-model calculations on the "thermal conductivity integrand" in Eq. (2) for NaCl.

[50] M. V. Klein, Phys. Rev. **131**, 1500 (1963).
[51] R. L. Rosenbaum, Ph.D. thesis, University of Illinois, 1968 (unpublished).

TABLE III. Summary of computer-fitted parameters.

Figure	Curve	Dopant	N_0[a] (mole%)	Y[b]	N[c] (mole%)	W[d]	ρ[e] (No./cm²)
4	*B*	Li^+	0.017	2.04×10^{-4}	0.0046	1.50×10^{-6}	4.32×10^{8}
4	*C*	Li^+	0.29	1.8×10^{-3}	0.038	1.35×10^{-6}	3.89×10^{8}
4	*D*	Li^+	0.67	8.1×10^{-3}	0.17	6.76×10^{-7}	1.94×10^{8}
5	*B*	Na^+	0.048	1.44×10^{-4}	0.010	1.50×10^{-6}	4.32×10^{8}
5	*C*	Na^+	0.59	36×10^{-4}	0.25	3.38×10^{-6}	9.75×10^{8}
5	*D*	Na^+	4.16	3.3×10^{-2}	2.32	7.50×10^{-7}	2.16×10^{8}
6	*B*	K^+	0.035	1.14×10^{-4}	0.047	6.76×10^{-7}	1.94×10^{8}
6	*C*	K^+	0.037[f]	9×10^{-4}	0.36	1.81×10^{-6}	5.9×10^{8}
7	*B*	Rb^+	0.0011	5.4×10^{-5}	0.0063	8.95×10^{-7}	2.6×10^{8}
7	*C*	Rb^+	0.024	2.64×10^{-4}	0.031	3.00×10^{-6}	8.65×10^{8}
8	*B*	Br^-	0.13	6.6×10^{-4}	0.27	7.50×10^{-8}	2.16×10^{7}
8	*C*	Br^-	1.70	3.6×10^{-3}	1.44	3.75×10^{-6}	1.08×10^{8}
9	*B*	I^-	0.061	2.34×10^{-4}	0.058	1.65×10^{-6}	4.75×10^{8}

[a] N_0 is dopant concentration determined by spectrochemical analysis.
[b] Y is computer-fitted value for point-defect scattering.
[c] N is calculated concentration by using S^2 and Y.
[d] W is computer-fitted value for dislocation scattering.
[e] ρ is calculated dislocation density by using Γ_0 and W.
[f] This result is unreliable because analysis was performed on only a small portion of the crystal where the impurity-concentration gradient is expected to be large.

occur in the region of the critical points where the phonon density of states is high. Ordinarily, such peaks are not simple resonances, because any resonance that would otherwise occur in this frequency region is strongly modified by the critical points. This situation is similar to the isotope-induced absorption case, and there is no thermal conductivity dip corresponding to absorption peaks of this type. Phonon resonance scatterings and their related optical absorptions are thoroughly discussed by Pohl[52] and Klein.[53]

We found impurity-induced absorption peaks in all the doped crystals except for rubidium. There the impurity concentration was perhaps too low to have detectable absorption peaks. The frequency range of the above absorption peaks could, in principle, cause conductivity dips in the observed temperature region. However, the thermal conductivity of the pure AgCl crystal decreases rapidly at temperatures above the maximum; thus it is very difficult to resolve any possible conductivity dips in this region. This suggests that the strength of phonon resonance scattering is weaker than that of phonon-phonon scattering. But, with high-impurity concentrations, resonance scattering may perhaps be revealed in a thermal conductivity curve.

In order to confirm this interpretation, a heavily Li^+-doped crystal was measured, and the conductivity shows a dip at 35°K in Fig. 15. This may be related to either one of the two absorption peaks at 69 ± 3 and 95 ± 2 cm^{-1}. A further discussion of this crystal is given in Sec. VII.

TABLE IV. Summary of point-defect scattering strength.

Dopant	$(\Delta M/M)^2$	$\Delta\beta/\beta$	$\Delta R/R$	$(\Delta\beta/\beta - 13.44(\Delta R/R))^2$	S^2[a]
Li^+	0.495	0.446	−0.076	2.14	4.775
Na^+	0.351	0.927	0.014	0.536	1.423
K^+	0.230	1.87	0.131	0.01	0.25
Rb^+	0.0244	1.75	0.178	0.416	0.856
Br^-	0.096	0.256	0.0461	0.0765	0.249
I^+	0.406	···	0.166	···	···

[a] $S^2=(\Delta M/M)^2+2[\Delta\beta/\beta-13.44\Delta R/R]^2$ [Eq. (6b)].

[52] R. O. Pohl, in *Localized Excitations in Solids*, edited by R. F. Wallis (Plenum Press, Inc., New York, 1968), p. 434.
[53] M. V. Klein, in *Physics of Color Centers*, edited by W. B. Fowler (Academic Press Inc., New York, 1968).

B. Temperature Region below Conductivity Maximum

Dislocations are probably the dominant phonon scattering mechanism at temperatures below the conductivity maximum in our crystals. The thermometer mounting technique produces two deformed regions near the knife edges, and these are constantly under the stress of the phosphor-bronze springs. This causes the dislocations which are generated in the deformed regions to propagate into the undeformed parts of the crystal. Such propagation of dislocations under stress has been observed in silver chloride by Sprackling.[54] From the computer fits for the impurity-doped crystals,

TABLE V. Summary of elastic constants and compressibilities used in this paper.

Crystal	Elastic constants (10^{11} dyn/cm²) C_{11}	C_{12}	C_{44}	Compressibility (10^{-12} cm²/dyn) β	Temperature (°K) T
LiCl[a]	6.074	2.27	2.692	2.82	4.2
NaCl[a]	5.733	1.123	1.331	3.76	4.2
KCl[b]	4.832	0.54	0.663	5.60	4.2
RbCl[a]	4.297	0.649	0.493	5.36	4.2
AgCl[c]	7.590	3.908	0.6894	1.95	4.2
AgBr[d]	5.63	3.30	0.720	2.45	300

[a] Reference 47.
[b] Reference 48.
[c] Reference 42.
[d] Reference 49.

[54] M. T. Sprackling, Phil. Mag. **13**, 1293 (1966).

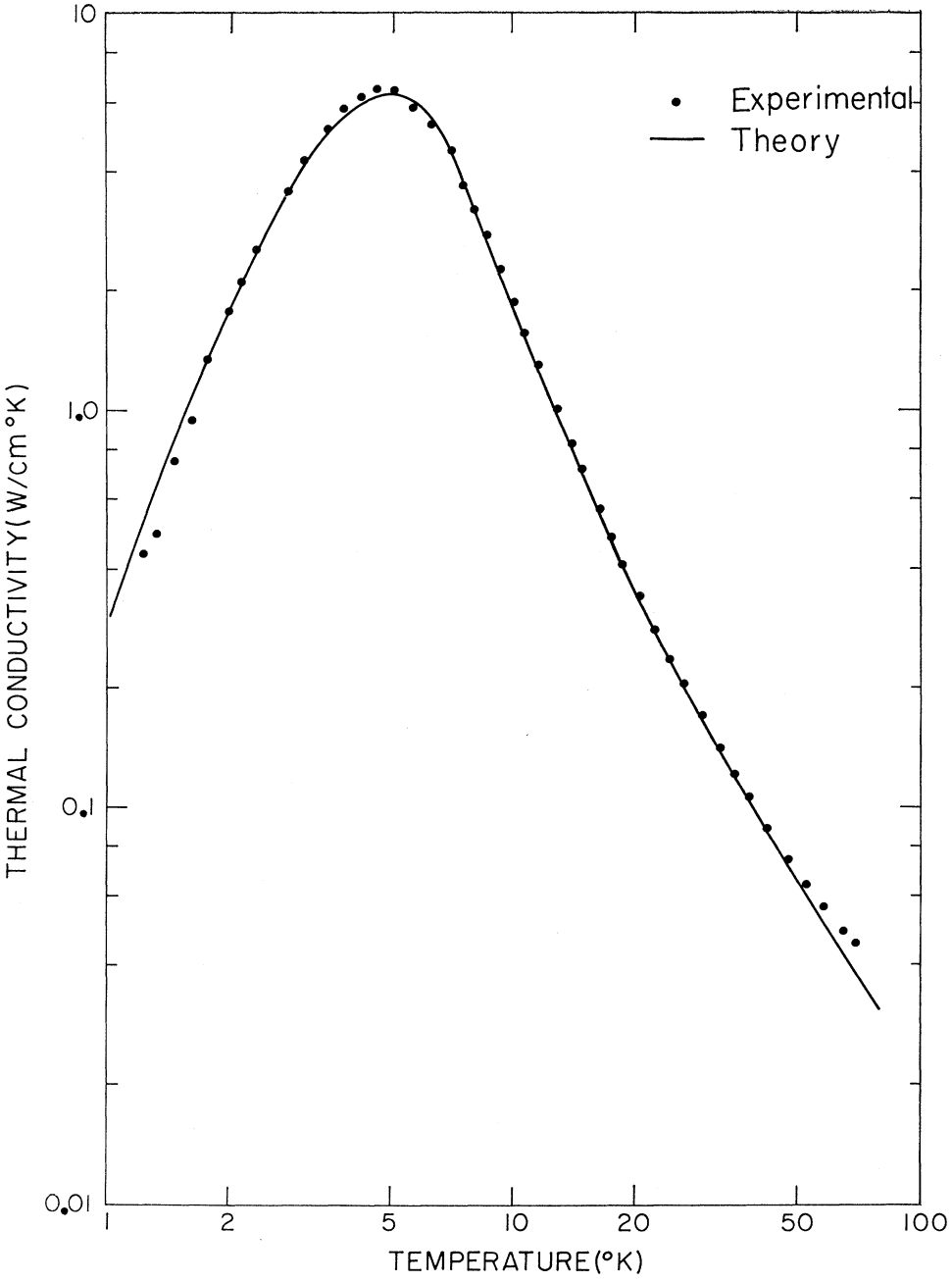

FIG. 14. Two-group-velocity model theoretical fit to the thermal conductivity data for pure silver chloride.

we may deduce a value for the dislocation density ρ by setting

$$\rho = W/\Gamma. \tag{11}$$

Expressions for Γ which have been derived by Klemens,[45] Carruthers,[46] and Ohashi[33] are

$$\Gamma_K = 6\times 10^{-2} b^2\gamma^2, \tag{12}$$

$$\Gamma_C = 1/192(gb\sigma/Dv^2), \tag{13}$$

$$\Gamma_0 = \tfrac{1}{2}(-g/c_{11})^2 b^2, \tag{14}$$

where b is the Burgers vector, γ is the Grüneisen constant, D is the mass density, v is the average group velocity, c_{11} is the elastic constant, g is the anharmonicity coefficient $\phi'''(r_0)$, r_0 is the lattice constant, $\sigma = (1-2\nu)/(1-\nu)$, and ν is the Poisson's ratio. The value of g is -2.2×10^{12} erg/cm^2, as obtained from Kurosawa's expression for the interionic potential for AgCl.[55] The values of the other parameters in Eqs. (12)–

[55] T. Kurosawa, J. Phys. Soc. Japan **13**, 153 (1958).

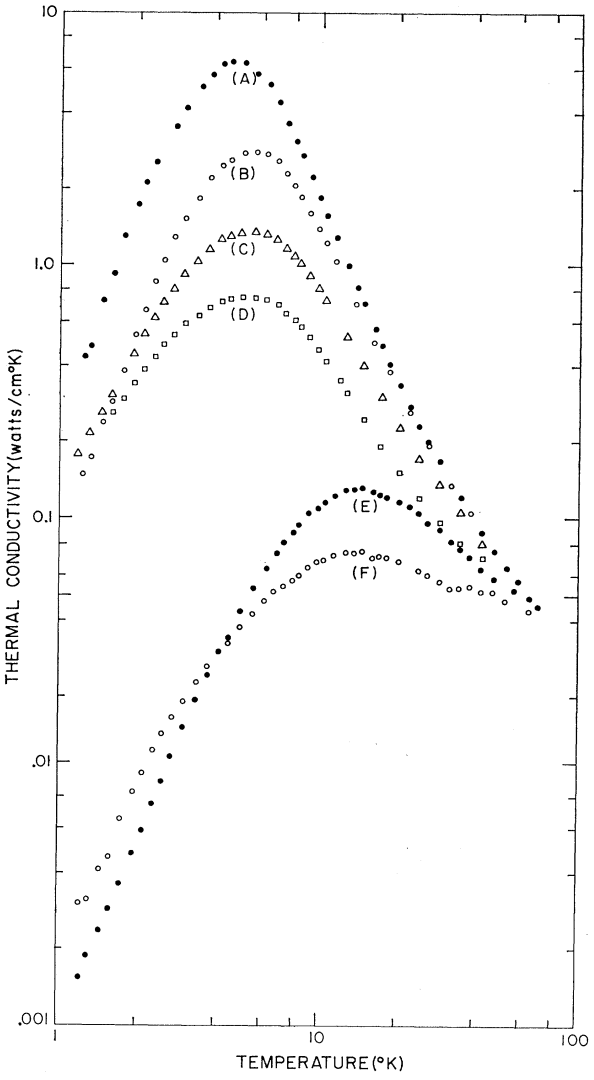

FIG. 15. Thermal conductivity data for silver chloride doped with lithium. Curve A, pure; curve B, 0.017 mole% of Li^+; curve C, 0.29 mole%; curve D, 0.67 mole%; curve E, 2.49 mole%, precipitated; curve F, quenched; curve E.

(14) are

$$b=\sqrt{2}r_0=3.88\times10^{-8}\text{ cm},\quad\text{(Ref. 56)}$$
$$\gamma=1.6,\quad\text{(Ref. 43)}$$
$$C_{11}=7.59\times10^{11}\text{ dyn/cm}^2,$$
$$C_{12}=3.908\times10^{11}\text{ dyn/cm}^2,$$
$$C^{44}=0.6894\times10^{11}\text{ dyn/cm}^2,$$
$$D=5.699\text{ g/cm}^3,$$
$$v=1.62\times10^5\text{ cm/sec}.$$

[56] M. N. Kabler, M. B. Miller, and L. M. Slifkin, J. Appl. Phys. **34**, 1953 (1963).

These give the following values for Γ:

$$\Gamma_K=2.30\times10^{-16}\text{ cm}^2,\quad(15)$$
$$\Gamma_C=9.04\times10^{-16}\text{ cm}^2,\quad(16)$$
$$\Gamma_0=6.33\times10^{-15}\text{ cm}^2.\quad(17)$$

Klemens has pointed out that random dislocations reduce the scattering rate by a factor of 0.55. Combining this with Ohashi's value in Eq. (17), we find the dislocation densities in the impurity-doped crystals range between $2.16\times10^7/\text{cm}^2$ and $9.75\times10^8/\text{cm}^2$. We also estimate the dislocation density in the heat-treated single crystals (see Sec. IV) to be approximately $10^7/\text{cm}^2$. We do not use the values for Klemens's and Carruthers's calculations, as they are probably somewhat low, if previous work in alkali halides is any guide. The above values of the dislocation density are felt to be reliable.

VII. OTHER CRYSTALS

A. Heavily Li^+-Doped Crystal

A heavily Li^+-doped crystal with an impurity concentration of 2.49 mole% in the melt was white and opaque after annealing. Its conductivity, shown in curve E in Fig. 15, is depressed by a factor of 300 with respect to the pure crystal at 1.5°K. The crystal became transparent when quenched to liquid-nitrogen temperature, but later turned milky and eventually became opaque. Immediately after quenching, the crystal was mounted in the cryostat and necessarily held at room temperature for more than 3 h while the system was pumped out. The resulting conductivity plotted as curve F shows an increase in the low-temperature region but is depressed both near and above the peak and exhibits a dip around 35°K.

The effects of annealing and quenching the heavily doped crystal may be explained in the following way: From the appearance of the annealed crystal, we conclude that most of the lithium ions were separated from the solid solution and formed clusters, which cause phonon scattering similar to that observed by Bausch *et al.*[24] For the quenched crystal, we expect only partial precipitation, with many of the lithium ions in substitutional sites. The conductivity reveals a typical resonance dip.

B. Copper-Doped Crystals

Two copper-doped crystals were annealed by our standard procedure to ensure that only cuprous ions were present in the crystals.[57,58] The solubility of cuprous chloride in silver chloride may be as high as 1% as suggested by Parasnis.[59] The more lightly doped

[57] F. Moser, R. N. Nail, and F. Urbach, J. Phys. Chem. Solids **3**, 153 (1957).
[58] F. Moser, N. R. Nail, and F. Urbach, J. Phys. Chem. Solids **9**, 217 (1959).
[59] A. S. Parasnis, Acta Met. **9**, 165 (1961).

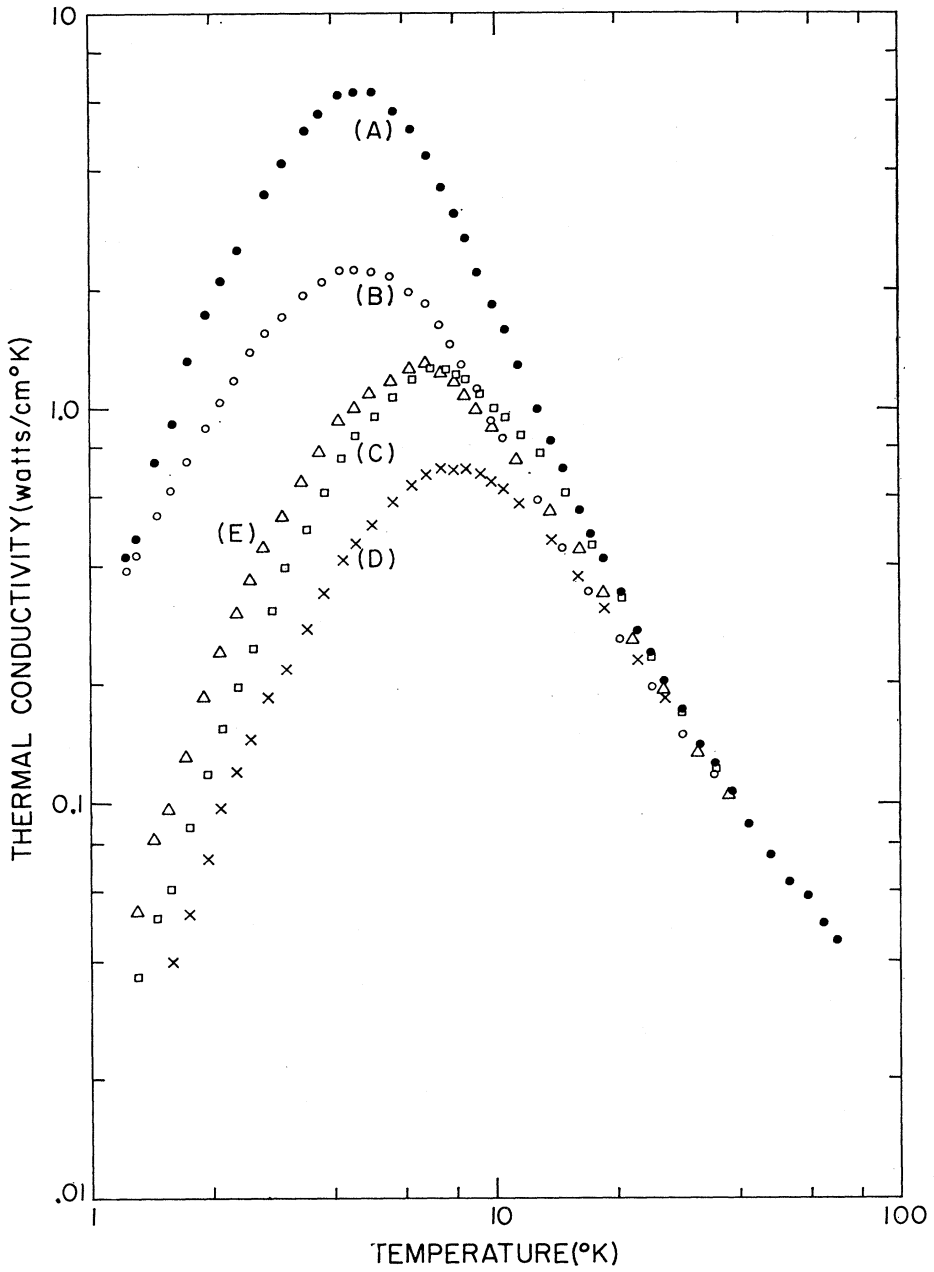

FIG. 16. Thermal conductivity data for silver chloride doped with copper. Curve A, pure; curve B, 0.065 mole% of Cu^{+}; curve C, 0.065 mole% of Cu^{++}; curve D, 0.80 mole% of Cu^{+}; curve E, 0.80 mole% of Cu^{++}.

crystal ($SH10$) was clear while the more heavily doped crystal ($SH24$) was milky. Their conductivities are shown in Fig. 16: Curve B is the data of $SH10$ in the cuprous state, and curve D is the data of $SH24$ in the cuprous state. Curve B peaks at 4.5°K and has a moderate depression above the maximum, but it does not have a low-temperature depression. Curve D, on the other hand, has a very large depression below the conductivity maximum along with a T^3 temperature dependence, but it does not exhibit a high-temperature depression.

After these measurements, the same crystals were annealed in a chlorine atmosphere for 10 h at 400°C and they were cooled to room temperature at a slow rate. This process converts the cuprous ions to cupric ions.[57,58] Both crystals appeared yellowish brown after the chlorination. Their conductivities are given by curves C and E in Fig. 16.

After the chlorination, both crystals have cupric precipitates. Curve C represents a lower Cu^{++} concentration than curve E. Thus, we expect curve C to be above curve E for all temperatures. However, curve C is below curve E on the low-temperature side of the conductivity maximum. This suggests that some additional scattering mechanism, possibly resonance scattering, may be present in curve C.

Cu^{++} is a paramagnetic ion which has the electronic configuration $3d^9$. Tucker[60] has observed three types of Cu^{++} centers in silver chloride: Type A has a bound vacancy at a nearest positive-ion site, type B has a vacancy at a next-nearest positive-ion site along the [100] direction, and type C is an isolated ion, which gives rise to a strong Jahn-Teller distortion along a cube edge of the surrounding octahedron of Cl^- ions. The hyperfine-splitting constants of these centers given by Tucker are of the order of 100 G, corresponding to an energy of the order of 10^{-2} cm^{-1} or 0.014°K. A splitting of this magnitude might give a thermal conductivity resonance dip below 10^{-2} °K, which is too low to have a strong effect in our present temperature range. Tucker pointed out that the type-C center is strongly affected by the Jahn-Teller distortion. Perhaps this could cause energy splittings of the order of a few wave numbers and thus perhaps be related to the depression in curve C. If the low-temperature depression of curve C is indeed due to this resonance scattering, then we must assume that curve-C crystals have more substitutional cupric ions in the lattice than do those of curve E. This situation could be explained in the following way: Both copper-doped crystals were chlorinated at 400°C and cooled to room temperature at a slow rate. The crystal $SH24$ (curve E) might have been supersaturated with cupric ions at high temperature, where the cupric ions could move relatively easily in the lattice. The precipitation rate would then be fast and a large density and elastic mismatch would form between the precipitates and the host. This could induce further migration of cupric ions to the precipitation sites. Therefore we would expect the crystal to be only slightly supersaturated at room temperature. On the other hand, it is reasonable to suppose that crystal $SH10$ (curve C) was not supersaturated until a much lower temperature, where the curpic ions would be relatively immobile in the lattice. This would allow the crystal to remain in a more highly supersaturated state than the heavily doped crystal, and hence there would be more substitutional cupric ions in the lattice for curve C than for curve E.

VIII. CONCLUSIONS

The thermal conductivity of pure and doped silver-chloride crystals has been measured as a function of temperature from 1.2 to 80°K. The far-infrared absorption of some of the impure crystals has also been measured from 33 to 105 cm^{-1} at 7°K.

[60] R. F. Tucker, Phys. Rev. 112, 725 (1958).

A. Pure Crystals

In the polycrystalline sample, the low-temperature part of the thermal conductivity curve is depressed probably due to the limitation of the phonon mean free path by the crystallite boundaries. The difference between the estimated phonon mean free path and the observed average grain size suggests that specular reflection within the grains or transmission through the grain boundaries occurs.

The results of surface treatments on a single crystal suggest that dynamical dislocation loops beneath the surface probably cause diffuse boundary scattering.

After a 10-h 400°C anneal, similar strengths of phonon scattering are introduced into the single crystals by various speeds of cooling. This scattering may be due to bare dislocations or dislocations surrounded by a Debye-Hückel cloud.

No far-infrared absorption peaks are observed in the pure crystal.

B. Doped Crystals

Simple point-defect Rayleigh scattering cannot explain the data obtained on the doped crystals. In order to fit the conductivity curves within the theoretical model used here, we have to assume that the doped crystals contain dislocations in large (10^8–10^9 cm^{-2}) densities. An independent determination of the dislocation densities would be desirable. The derivations from Rayleigh scattering observed in the high-concentration crystals may be due to resonance scattering by impurity modes. Only in the quenched, heavily lithium-doped crystal is a well defined thermal conductivity dip at 35°K observed. In the same crystal, a strong low-temperature depression shows typical phonon scattering by precipitates.

For the copper-doped crystals, the thermal conductivity suggests a resonance below 1°K, which possibly is due to Jahn-Teller distortion about isolated Cu^{++} ions.

As for the far-infrared absorption data of the doped crystals, more information on the phonons in the silver-chloride lattice is needed in order to perform a significant analysis of the absorption spectra.

ACKNOWLEDGMENTS

We wish to thank Dr. H. F. Macdonald for help with the infrared measurements and Dr. P. R. Vijayaraghavan and Dr. R. M. Nicklow for the use of their neutron data. Thanks are also due to Professor L. Slifkin for suggesting the purification technique used on AgCl.